HHS Public Access

Author manuscript

Int J Cardiovasc Imaging. Author manuscript; available in PMC 2022 February 01.

Published in final edited form as:

Int J Cardiovasc Imaging. 2021 February ; 37(2): 651–661. doi:10.1007/s10554-020-02038-6.

Aortic annular dimensions by non-contrast MRI using k–t accelerated 3D cine b-SSFP in pre-procedural assessment for transcatheter aortic valve implantation: a technical feasibility study

Pascale Aouad[1], **Kelly Brooke Jarvis**[1], **Marcos Ferreira Botelho**[1], **Ali Serhal**[1], **Julie Blaisdell**[1], **Louise Collins**[1], **Shivraman Giri**[2], **Daniel Kim**[1], **Michael Markl**[1], **Mark J. Ricciardi**[3], **Charles J. Davidson**[3], **Jeremy Collins**[1], **James Carr**[1]

[1]Department of Radiology, Department of Medicine, Feinberg School of Medicine, Northwestern University, 676 N St Clair (Arkes) suite 800, Chicago, IL 60611, USA

[2]Siemens Healthcare, Chicago, IL, USA

[3]Department of Cardiology, Department of Medicine, Feinberg School of Medicine, Northwestern University, Chicago, IL, USA

Abstract

To evaluate k–t accelerated 3D cine b-SSFP (balanced steady state free precession) as magnetic resonance imaging (MRI) technique for aortic annular area measurement in transcatheter aortic valve replacement (TAVR) planning compared to computed tomography angiography (CTA) and other non-contrast MRI sequences with reduced imaging time and without contrast administration. 6 volunteers and 7 TAVR candidates were prospectively enrolled. The volunteers underwent an MRI while TAVR candidates underwent an MRI and CTA. The following non-contrast MRI sequences were obtained at the level of the aortic root: 2D cine b-SSFP [GRAPPA (GeneRalized Autocalibrating Partially Parallel Acquisitions), R = 2], 3D cine b-SSFP [GRAPPA R = 2], navigator triggered 3D b-SSFP MRA [GRAPPA, R = 2] and k–t accelerated 3D cine b-SSFP [PEAK GRAPPA, R = 5]. Qualitative analysis and aortic annular area measurements in systole and diastole were obtained. k–t accelerated 3D cine b-SSFP provided image quality that is acceptable for confident diagnosis with very good interrater agreement. There was no statistically significant difference in aortic annular measurements between k–t accelerated 3D cine b-SSFP and CTA or other MRI sequences ($p > 0.05$). Bland–Altman analysis showed no systemic difference of annular area measurements between k–t accelerated 3D cine b-SSFP and each of the other techniques. There was excellent interrater agreement on aortic annular area measurements during systolic (ICC = 0.976, $p < 0.001$) and diastolic (ICC = 0.971, $p < 0.001$) phases using k–t accelerated 3D cine b-SSFP. K–t accelerated 3D cine b-SSFP is a promising alternative for the assessment of annular sizing in pre-TAVR evaluation while offering a reasonable combination of imaging parameters during one breath-hold.

✉Pascale Aouad, pascale.aouad@northwestern.edu.

Conflict of interest The authors declare that they have no conflict of interest.

Ethics approval This study has been performed in accordance with the local ethics committee.

Keywords

Transcatheter aortic valve replacement; Severe aortic stenosis; Non-contrast magnetic resonance imaging; Computed tomography angiography; k–t acceleration

Introduction

Transcatheter aortic valve replacement (TAVR) is now well established for the treatment of severe symptomatic aortic valve stenosis in patients at heightened risk for complications during surgical aortic valve replacement [1]. Pre-procedural imaging is necessary for determining anatomic suitability and for selecting the optimal prosthetic valve size and vascular approach. Computed tomographic angiography (CTA) plays a crucial role in the assessment of aortic annular size, aortic root anatomy and vascular access; however, the need for iodinated contrast media administration presents a major drawback in a large subset of patients who are typically elderly, sick, and have poor kidney function.

Several studies have demonstrated the reproducibility of non-contrast MRI in the assessment of aortic root anatomy and annulus measurements using multi-slice, 2D cine balanced steady-state free-precession (b-SSFP) [1–4]. However, the multi-slice 2D cine b-SSFP technique requires careful slice positioning (e.g., orthogonal to the aortic root long axis) and repetitive breath-hold acquisitions to cover the entire aortic root and thus may suffer from inaccuracies in slice orientation and mis-registration between acquired slices. To overcome these limitations, recent publications reported the applicability of 3D acquisitions in pre-TAVR assessment, including 3D-FLASH magnetic resonance angiography (MRA) [5] and free-breathing (i.e. self-navigated and navigator-gated) 3D b-SSFP [4, 6–8]. These methods have the advantage of generating isotropic spatial resolution and reformatting in any orientation but can require long scan times which is problematic in this population group (i.e. typically elderly patients with multiple medical conditions) and thus are limited regarding imaging coverage and resolution.

Given that the majority of patients undergoing TAVR are elderly and sick, a tolerable and relatively short exam time is particularly important to improve patient's comfort and cooperation. The application of k–t acceleration to 3D cine b-SSFP MRI provides faster imaging (i.e. acceleration factor, R = 5 versus R = 2 for conventional techniques) and thus the potential for an improved imaging acquisition within a single breath-hold. The purpose of this study is to assess the feasibility of non-contrast k–t accelerated 3D cine b-SSFP for aortic root analysis in comparison to conventional MRI sequences (2D cine b-SSFP, 3D cine b-SSFP and navigator-triggered 3D b-SSFP MRA) and to the gold standard CTA.

Materials and methods

Study population

This prospective study was approved by our institutional review board. Informed consent was obtained from each subject prior to the investigation in accordance with local ethics committee requirements. The study included 6 healthy volunteers (6 males; mean age 56 years, [range 24–75 years]) and 7 patients (4 males; mean age 72 years, [range 57–80 years])

with severe aortic stenosis referred for pre-TAVR evaluation. All the studied subjects underwent non-contrast-enhanced cardiac MRI and the 7 TAVR candidates also underwent the clinically indicated CTA for pre-procedure planning.

Image acquisition and reconstruction

All the cardiac MRIs were performed on a 1.5T MRI Scanner (MAGNETOM Aera, Siemens Healthcare, Erlangen, Germany) without contrast administration. The prototype k–t accelerated 3D cine b-SSFP was compared to each of the following conventional sequences: 2D cine b-SSFP, 3D cine b-SSFP and navigator-triggered 3D b-SSFP MRA, the latter was obtained as two different scans one during a diastolic phase and the other during a systolic phase. All of these sequences were acquired orthogonal to the aortic root and to sample the aortic root including the aortic annulus. Figures 1 and 2 show the orientation and position of the plane of imaging as well as the length of coverage for 2D cine b-SSFP and for all the 3D sequences respectively. Table 1 shows the typical imaging parameters for each of these sequences. In addition to the cardiac MRI, quiescent-interval single-shot unenhanced MRA of the abdominopelvic arterial vasculature was obtained to visualize the vascular access.

All the CTAs were performed on a dual source scanner (SOMATOM Flash, Siemens Healthcare, Erlangen, Germany) according to the conventional protocol used in our institution with retrospective ECG-gated CT angiogram of the heart followed by a FLASH CTA of the thoracoabdominal aorta and pelvic vessels.

Description of the k–t Accelerated 3D cine b-SSFP

This imaging sequence utilized PEAK-GRAPPA [9], an extension of k–t GRAPPA [10], in combination with b-SSFP imaging [11, 12]. Briefly, PEAK-GRAPPA utilizes the parallel imaging technique of generalized autocalibrating partially parallel acquisitions (GRAPPA) [13] with undersampling also in the time dimension. As dynamic imaging exhibits a high degree of signal correlation in k-space and over time, it is possible to acquire a reduced amount of data (i.e. allowing for a reduced scan time) and then recover the missing portion of data retrospectively [10]. PEAK-GRAPPA has been used to substantially reduce scan times in 4D flow MRI [14, 15]. The k–t accelerated 3D cine b-SSFP imaging sequence was developed in-house based on an existing sequence with PEAK-GRAPPA that was then modified to have the high blood-tissue contrast of b-SSFP. The imaging parameters for this study are described in Table 1.

Image analysis

Cardiac MRI and CTA images were analyzed using 3D post-processing on a dedicated software (Horos project, Nimble Co LLC d/b/a Purview in Annapolis, MD USA) allowing free navigation and image plane selection. The aortic annulus was defined as a virtual ring passing through the basal hinge points of the three aortic valve cusps.

Qualitative analysis: The conspicuity of the aortic annulus and image quality were subjectively rated independently by two radiologists according to a 5-point scale: (1) not assessable/inadequate for diagnosis; (2) poor/marginally accepted for diagnosis; (3) fair/

acceptable for confident diagnosis; (4) good/adequate for confident diagnosis; (5) excellent/highly confident diagnosis.

Quantitative analysis: Two radiologists independently measured aortic annular area by manually drawing the contours of the annulus on the obtained plane during the middiastolic phase and during the systolic phase corresponding to the greatest valve opening. Both radiologists were blinded to other's measurements and to the results of CTA.

The contours of the aortic annulus were drawn in an ellipsoid fashion on both MRI and CTA ignoring any calcifications protruding into the lumen.

Figure 3 demonstrates the process of multiplanar reconstruction and the choice of the annulus plane on 3D acquisitions.

We compared the aortic annulus area measurements during diastole and systole obtained by the k–t accelerated 3D cine b-SSFP to the measurements obtained with each of the conventional MRI sequences (2D cine b-SSFP; 3D cine b-SSFP; navigator triggered 3D b-SSFP MRA) on all the recruited subjects as well as to the gold standard CTA on the TAVR candidates.

Statistical analysis

Statistical analysis was performed using Stata 14 (StataCorp, College Station, TX). Friedman test and post-hoc Wilcoxon signed ranks test were used to evaluate for difference in conspicuity and image quality across the four MRI sequences. Bonferroni adjusted alpha level of 0.017 per test (0.05/3) was used to interpret statistical significance of Wilcoxon signed ranks test. The normality of the data was verified using the Shapiro-Wilk test. Normally distributed variables were compared using paired *t* test. The correlation of annular measurements was assessed using Pearson analysis and the agreement of measurements was analyzed using Bland Altman.

Interrater agreement for conspicuity and image quality was analyzed using kappa test (κ). Kappa is interpreted as follows: $\kappa < 0.2$: poor agreement; $\kappa = 0.2–0.4$: fair agreement; $\kappa = 0.4–0.6$: moderate agreement; $\kappa = 0.6–0.8$: good agreement; $\kappa = 0.8 - 0.1$: very good agreement. Absolute-agreement, two-way mixed-effects model intraclass correlation coefficient (ICC) was used to analyze agreement of measurements between the two raters. ICC is interpreted as follows: < 0.5: poor; 0.5–0.75: moderate; 0.75–0.9: good; > 0.9 excellent.

Results

The images obtained with k–t accelerated 3D cine b-SSFP as well as with the other obtained MRI sequences (2D cine b-SSFP, 3D cine b-SSFP and navigator triggered 3D b-SSFP MRA) were of sufficient diagnostic quality for analysis of the aortic root in all the studied subjects. Aortic annulus conspicuity and image quality were significantly better on 2D cine compared to k–t accelerated 3D cine b-SSFP for both raters and image quality was better on 3D cine compared to k–t accelerated 3D cine b-SSFP for rater 1. No significant difference in annular conspicuity or image quality was seen between k–t accelerated 3D cine b-SSFP and

navigator-triggered 3D b-SSFP MRA. However, k–t accelerated 3D cine b-SSFP provided images that are fair/acceptable for confident diagnosis based on the subjective scoring of the conspicuity of the aortic annulus and image quality (Table 2).

K–t accelerated 3D cine b-SSFP was acquired within a single breath-hold in all the studied subjects with a mean time of acquisition of 18 s (14–28 s) and length of coverage of 24 mm. By comparison, 2D cine b-SSFP was obtained with 3 slices each of 5 mm mean thickness (4–6 mm) requiring a breath-hold and a mean acquisition time of 17 s (11–24 s) which requires an average of 51 s (33–72 s) to acquire the 3 slices covering a mean of 15 mm (12–18 mm); 3D cine b-SSFP was acquired within a single breath hold with 20 s (17–26 s) time of acquisition and a mean of 29 mm (18–32 mm) length of coverage; and navigator triggered 3D b-SSFP MRA was imaged during free breathing with navigator triggering and required 122 s (57–240 s) acquisition time for each of the systolic and diastolic phases with a mean length of coverage of 38.6 mm (28–55.5 mm). Figure 4 shows the annular area measured during systole and diastole on each of the MRI sequences in a TAVR candidate patient. Figure 5 shows the annular area measurements in a TAVR candidate subject on k–t accelerated 3D b-SSFP and CTA during systolic and diastolic phases.

The mean systolic annular area was not significantly different between the new sequence and the CTA as well as between the new sequence and each of the other MRI sequences: 2D cine b-SSFP, 3D cine b-SSFP and navigator triggered 3D b-SSFP MRA during both systole and diastole. The mean and standard deviation of annular area measurements obtained during systolic and diastolic phases are shown for all the obtained MRI sequences in all the studied subjects as shown in Table 3 and for k–t accelerated 3D cine b-SSFP and CTA in the TAVR candidates as shown in Table 4.

According to Pearson analysis, there was an excellent correlation of systolic area measurements between k–t accelerated 3D cine b-SSFP and the conventional MRI techniques (2D cine: $r = 0.89$ for rater 1 and $r = 0.89$ for rater 2; 3D cine: $r = 0.95$ for rater 1 and $r = 0.95$ for rater 2; navigator-triggered 3D b-SSFP MRA: $r = 0.90$ for rater 1 and $r = 0.92$ for rater 2; $p < 0.01$ for all data) and with CTA ($r = 0.99$ for rater 1 and $r = 0.98$ for rater 2; $p < 0.01$). Similarly, there was very good correlation of diastolic area measurements between k–t accelerated 3D cine b-SSFP and the conventional sequences (2D cine: $r = 0.96$ for rater 1 and $r = 0.97$ for rater 2, 3D cine: $r = 0.96$ for rater 1 and $r = 0.94$ for rater 2, navigator-triggered 3D b-SSFP MRA: $r = 0.95$ for rater 1 and $r = 0.95$ for rater 2; $p < 0.01$ for all data) and CTA ($r = 0.99$ for rater and $r = 0.99$ for rater 2; $p < 0.01$).

Bland–Altman analysis demonstrated no systematic difference in area measurements between the k–t accelerated 3D cine b-SSFP and the other MRI sequences during systole for both observers (Fig. 6). There was no systematic difference in area measurements between the k–t accelerated 3D cine b-SSFP and CTA during systolic and diastolic phases for both observes (Fig. 7).

There was at least moderate agreement between the raters on qualitative analysis of aortic annulus conspicuity and image quality (Table 5). There was excellent inter-rater agreement on aortic annular area measurements during systolic (ICC = 0.976, $p < 0.001$; 95%

confidence interval = 0.923–0.992) and diastolic (ICC = 0.971, $p < 0.001$; 95% confidence interval = 0.910–0.991) phases using k–t accelerated 3D cine b-SSFP. Excellent agreement was as well observed with 2D cine, 3D cine and navigator triggered 3D b-SSFP MRA.

Discussion

Our study shows the technical feasibility of k–t accelerated 3D cine b-SSFP in the assessment of the aortic annulus for pre-procedural TAVR planning which is fundamental to ensure optimal prosthesis choice and to reduce the risk of post procedural complications. The studied MRI sequence provided images that are acceptable for confident diagnosis during a breath-hold with reasonable temporal resolution and high isotropic spatial resolution allowing easy image data reformat and therefore resulting in reliable annular measurements. Acquisition time is reduced by comparison to 2D cine b-SSFP, which was obtained using 3 contiguous slices requiring 3 breath-holds during a total mean time of 51 s to cover 15 mm, without significant drawback on temporal resolution, length of coverage or in-plane spatial resolution. Slice thickness is dramatically improved by comparison to 3D cine b-SSFP (1.5 mm with the study sequence compared to 5 mm with 3D cine b-SSFP). Acquisition time and temporal resolution are largely improved by comparison to navigator triggered 3D b-SSFP MRA which requires a mean time of acquisition of 122 sec to cover a mean of 38.6 mm.

A large subset of patients undergoing TAVR are usually elderly, sick, and have poor kidney function. Therefore, an imaging modality that can offer short scanning time and tolerable exam without the need for contrast administration is beneficial. Using k–t accelerated 3D cine b-SSFP, non-contrast MRI can be implemented as a potential alternative to the current exam of choice, CTA, in suitable patients undergoing TAVR evaluation without the administration of contrast and without exposure to radiation, the latter can be of relevant importance with the expanding application of TAVR into younger population.

Recent studies have investigated non-contrast MRI for aortic annular sizing in TAVR and reported, in agreement to our study, that non contrast MRI can provide annular measurements similar to the traditionally adopted imaging modalities for TAVR planning as echocardiography and CTA. La Manna et al. [1] demonstrated good correlation between transthoracic echocardiography and non-contrast MRI using 2D cine b-SSFP in aortic annulus measurements but with a tendency to report larger values with MRI than transthoracic echocardiography. Similarly, Paelinck et al. [2] reported excellent agreement in aortic annular measurement between MRI using 2D cine b-SSFP and transesophageal echocardiography but a tendency to underestimate by transthoracic echocardiography in comparison to MRI and transesophageal echocardiography. Ruile et al. [5] evaluated respiratory navigated 3D gradient echo FLASH sequence acquired during diastole and demonstrated agreement for prosthesis sizing between systolic CTA and modelled systolic MRA. An overall excellent image quality was obtained which was attributed to respiratory navigation avoiding respiratory motion and to the static acquisition during diastole allowing for less arrhythmia related image deterioration. However, the acquisition time is long (mean acquisition time = 14 ± 4.2 min) and this sequence is not temporally resolved and provides images only during diastole, therefore the systolic annular measurements were modelled

using a corrective factor derived from the difference in the CTA dimensions between systolic and diastolic phases which can be a potential source of error. In accordance with our results, Koos et al. [6] reported close but not identical aortic annular measurements between navigator-gated 3D b-SSFP whole heart acquisition, dual source CTA and transesophageal echocardiography based on annular diameter on coronal and sagittal views. Other authors demonstrated similar annular measurements between free-breathing self-navigated 3D sequence and 2D cine b-SSFP in 10 healthy subjects with a mean acquisition length of 22.6 ± 1.2 cm and mean scan time of 6.4 ± 1.3 min for free-breathing self-navigated 3D compared to 10.4 ± 3.7 min scan time for 2D cine acquisitions of the LVOT, aortic valve and root. The authors reported however significantly higher noise for the free-breathing self-navigated 3D but this was compensated by a higher contrast to noise ratio [8]. Despite the previously described potential role of non-contrast MRA in pre-TAVR evaluation, none of these techniques has been adopted into clinical practice which may be due to limitations related to the long acquisition times requiring patient's cooperation with shorter scan times being achievable at the expense of decreased field of coverage, lower temporal or spatial resolutions. Therefore, k–t accelerated 3D cine b-SSFP with an acceleration factor of 5 can address these limitations ensuring reduced scan time with reasonable spatial and temporal resolutions and appropriate coverage and may represent a robust technique for alternative imaging in a subset of subjects.

Our study has some limitations. The sample size was limited however our aim was to demonstrate the feasibility of the k–t accelerated 3D cine b-SSFP in pre-TAVR aortic root evaluation and further validation is required with larger study population. Only aortic annular area was reported however other potentially relevant anatomic parameters such as the distance of the coronary ostia to the annulus and the diameter of the aortic root were not measured as these were not always included in the field of view of all the acquired sequences. Although the length of coverage was comparable to the other MRI sequences, a larger coverage is still desirable to include more anatomic landmarks and expand the analysis. Assessment of the amount of aortic valve and vessel calcifications and the potential interference with the image quality was not evaluated. These issues can be addressed in future larger studies. Continuous b-SSFP sequences have potential considerations for specific absorption rate and higher flip angles may need to be adjusted to meet clinical operating mode requirements. Note that the k–t accelerated 3D cine b-SSFP sequence was not an extension of the other tested 3D cine b-SSFP sequence but rather developed in-house based on another sequence with k–t acceleration. It was not the aim of the study to systematically compare these techniques (i.e. 3D cine b-SSFP with and without k–t acceleration) but rather to test the utility of the newly developed sequence. Nevertheless, our study illustrated the feasibility of the k–t accelerated 3D cine b-SSFP technique and future studies are warranted to optimize the MRI protocol for TAVR planning.

Conclusions

We demonstrated in this preliminary study the feasibility of k–t accelerated 3D cine b-SSFP MRI for pre-TAVR aortic annular assessment with resultant images of diagnostic quality and comparable measurements to the previously described MRI sequences and CTA. The studied accelerated MRI technique is a potential alternative to CTA for pre procedure planning in

TAVR patients by providing a single breath-hold 3D cine acquisition with adequate imaging coverage of the aortic annulus and an optimal combination of spatial and temporal resolution. This protocol can be combined with non-contrast MRA of the abdomen/pelvis/lower extremities to potentially provide a comprehensive non contrast MRI protocol for TAVR planning that may be used as an alternative approach for patients that are not suitable candidates for CTA.

Funding

This work was supported by the National Institute of Health [Grant Numbers NHLBI T32 HL134633].

References

1. La Manna A, Sanfilippo A, Capodanno D, Salemi A, Polizzi G, Deste W et al. (2011) Cardiovascular magnetic resonance for the assessment of patients undergoing transcatheter aortic valve implantation: a pilot study. J Cardiovasc Magn Reson 13:82 [PubMed: 22202669]
2. Paelink BP, Van Herck PL, Rodrigus I, Claeys MJ, Laborde J-C, Parizel PM (2011) Comparison of magnetic resonance imaging of aortic valve stenosis and aortic root to multimodality imaging for selection of transcatheter aortic valve implantation candidates. Am J Cardiol 108:92–98 [PubMed: 21529729]
3. Jabbour A, Ismail TF, Moat N, Gulati A, Roussin I, Alprendurada F et al. (2011) Multimodality imaging in transcatheter aortic valve implantation and post-procedural aortic regurgitation comparison among cardiovascular magnetic resonance, cardiac computed tomography, and echocardiography. J Am Coll Cardiol 58(21):2165–2173 [PubMed: 22078422]
4. Cannaò PM, Muscogiuri G, Schoepf UJ, De Cecco CN, Suranyi P, Lesslie VW et al. (2017) Technical feasibility of a combined noncontrast magnetic resonance protocol for preoperative transcatheter aortic valve replacement evaluation. J Thoracic Imaging 00:1–8
5. Ruile P, Blanke P, Krauss T, Dorfs S, Jung B, Jander N (2016) Pre-procedural assessment of aortic annulus dimensions for transcatheter aortic valve replacement: comparison of a non-contrast 3D MRA protocol with contrast-enhanced cardiac dual-source CT angiography. Eur Heart J Cardiovasc Imaging 17:458–466 [PubMed: 26219296]
6. Koos R, Altiok E, Mahnken AH, Neizel M, Dohmen G, Marx N et al. (2012) Evaluation of aortic root for definition of prosthesis size by magnetic resonance imaging and cardiac computed tomography: implications for transcatheter aortic valve implantation. Int J Cardiol 158:353–358 [PubMed: 21315460]
7. Gopal A, Grayburn PA, Mack M, Chacon I, Kim R, Montenegro D et al. (2015) Noncontrast 3D CMR imaging for aortic valve annulus sizing in TAVR. JACC Cardiovasc Imaging 8:375–378 [PubMed: 25772841]
8. Renker M, Varga-Szemes A, Schoepf UJ, Baumann S, Piccini D, Zenge MO et al. (2016) A non-contrast self-navigated 3-dimensional MR technique for aortic root and vascular access route assessment in the context of transcatheter aortic valve replacement: proof of concept. Eur Radiol 26:951–958 [PubMed: 26188657]
9. Jung B, Ullmann P, Honal M, Bauer S, Hennig J, Markl M (2008) Parallel MRI with extended and averaged GRAPPA Kernels (PEAK-GRAPPA): optimized spatiotemporal dynamic imaging. J Magn Reson Imaging 28:1226–1232 [PubMed: 18972331]
10. Huang F, Akao J, Vijayakumar S, Duensing GR, Limkeman M (2005) K-t GRAPPA: A k-space Implementation for dynamic MRI with high reduction factor. Magn Reson Med 54:1172–1184 [PubMed: 16193468]
11. Scheffler K, Lehnhardt S (2003) Principles and applications of balanced SSFP techniques. Eur Radiol 13:2409–2418 [PubMed: 12928954]
12. Markl M, Leupold J (2012) Gradient echo imaging. J Magn Reson Imaging 35:1274–1289 [PubMed: 22588993]

13. Griswold MA, Jakob PM, Heidemann RM, Nittka M, Jellus V, Wang J, Kiefer B, Haase A (2002) Generalized autocalibrating partially parallel acquisitions (GRAPPA). Magn Reson Med 47:1202–1210 [PubMed: 12111967]

14. Schnell S, Markl M, Entezari P, Mahadewia RJ, Semaan E, Stankovic Z et al. (2014) K-t GRAPPA accelerated four-dimensional flow MRI in the aorta: effect on scan time, image quality, and quantification of flow and wall shear stress. Magn Reson Med 72:522–533 [PubMed: 24006309]

15. Bollache E, Barker AJ, Dolan RS, Carr JC, Ooij PV, Ahmadian R (2018) k-t accelerated aortic 4D flow MRI in under two minutes: Feasibility and impact of resolution, k-space sampling patterns, and respiratory navigator gating on hemodynamic measurements. Magn Reson Med 79:195–207 [PubMed: 28266062]

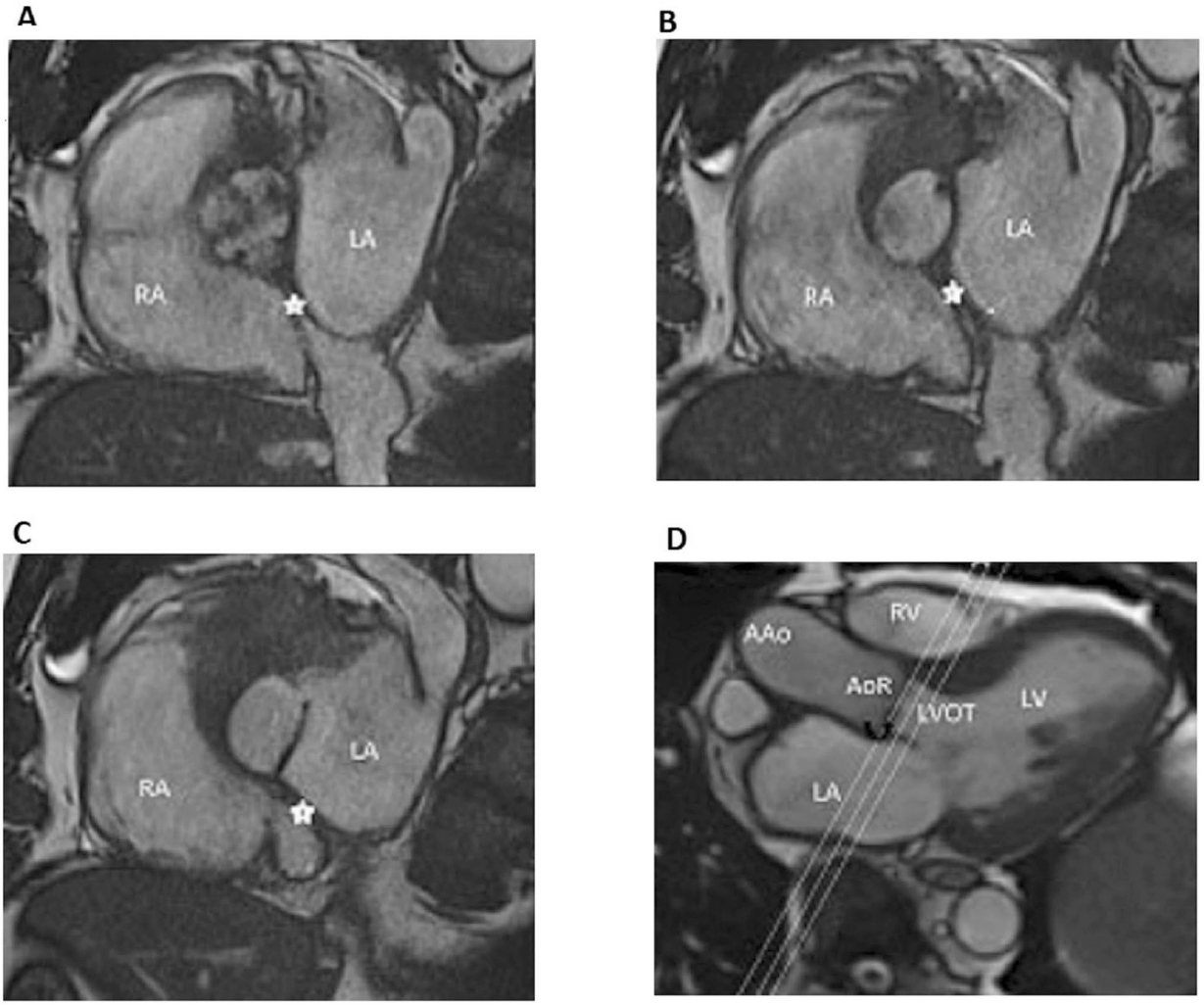

Fig. 1.

Plane position and orientation for 2D cine b-SSFP. The planes of the three acquired slices of 2D cine b-SSFP (**a**–**c**) are shown by cross-reference to a 3-chamber cine view (**d**). Note that the slices are acquired in a plane orthogonal to the aortic root covering the aortic annulus and part of the aortic root and LVOT. In this case, the image **b** represents the best slice position to choose for aortic annulus measurement as it passes through the most caudal aspect of the aortic valve leaflets. *AAo* ascending aorta, *AoR* aortic root, *LA* left atrium, *LV* left ventricle, *LVOT* left ventricular outflow tract; *RA* right atrium, *RV* right ventricle. The black curved arrow **d** points toward the aortic valve and the star (**a**–**c**) indicates the interatrial septum

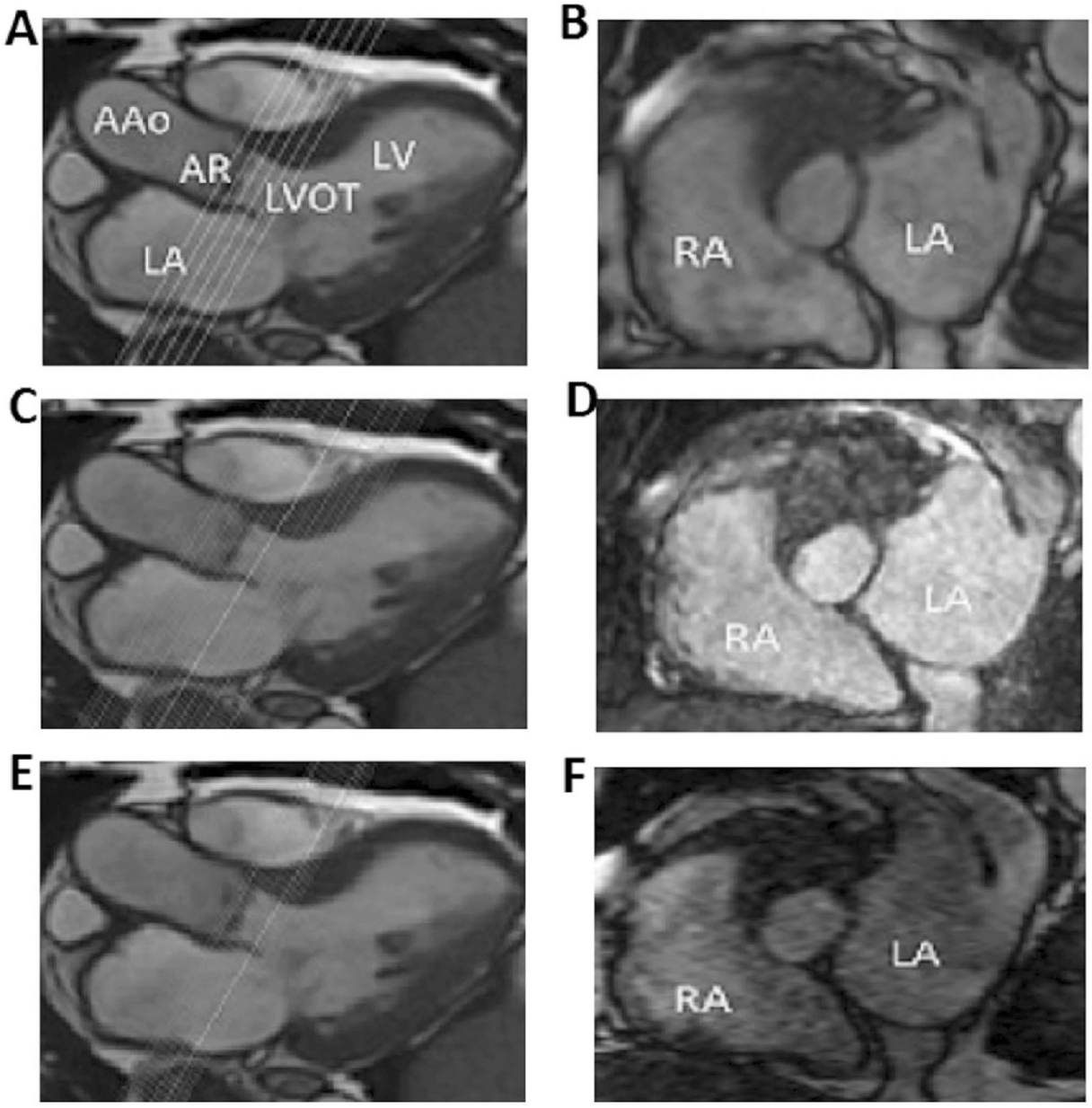

Fig. 2.

Plane position and orientation and length of coverage for the 3D sequences. The planes of the acquired slices of 3D cine b-SSFP (**b**), navigator triggered 3D b-SSFP MRA (**d**) and k–t accelerated 3D cine b-SSFP (**f**) are shown by cross-reference to 3-chamber cine view (**a**, **c**, **e**). Note that the slices are acquired in a plane orthogonal to the aortic root covering the aortic annulus and part of the aortic root and LVOT. Similar length of coverage can be appreciated between 3D cine b-SSFP and k-t accelerated 3D cine b-SSFP (**a** and **e**) but a wider coverage is seen for the navigator triggered 3D b-SSFP MRA (**c**) as shown by cross-reference to the 3D cine. Similar slice thickness can be seen between navigator triggered 3D b-SSFP MRA and k-t accelerated 3D cine b-SSFP (**c** and **e**) however obviously thicker slices are demonstrated with 3D cine b-SSFP. Note that the navigator triggered 3D b-SSFP MRA

is not time resolved and is acquired during a single cardiac phase. *AAo* Ascending aorta, *AR* aortic root, *LA* left atrium, *LV* left ventricle, *LVOT* left ventricular outflow tract, *RA* right atrium

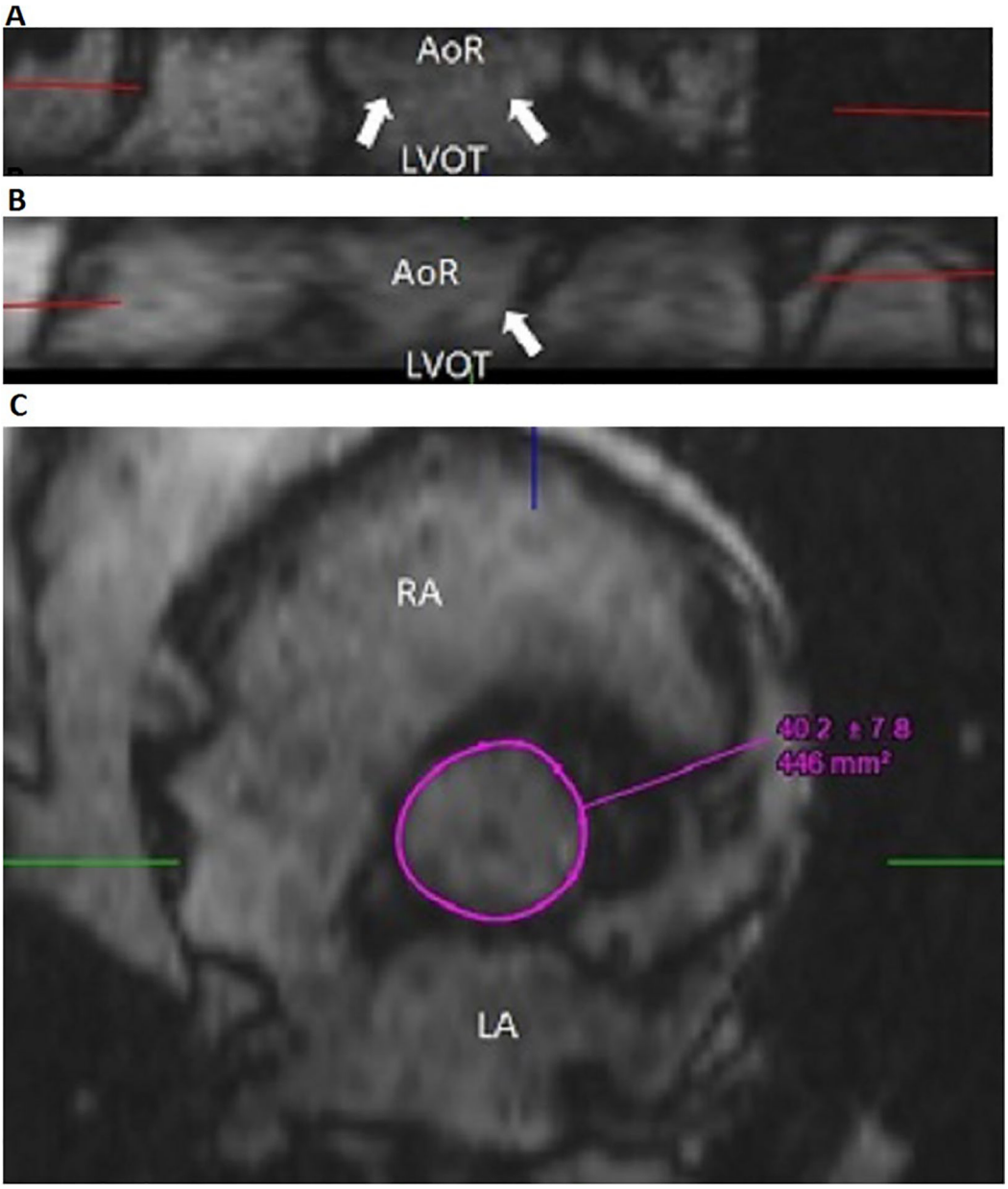

Fig. 3.

Multiplanar reformat in the aortic annulus plane for k–t accelerated 3D cine b-SSFP. Multiplanar reconstruction of the 3D dataset from k–t accelerated 3D cine b-SSFP allows reconstruction in any plane and therefore the plane of imaging can be adjusted to pass by the hinge points of the three aortic leaflets, referred to by the white arrows on coronal and sagittal reconstructions (**a** and **b**), which corresponds to the plane of the aortic annulus. 3D acquisition is therefore less dependent on appropriate slice orientation chosen during scanning by comparison to the 2D acquisition given the potential of plane adjustment by 3D reconstruction. Manual drawing of the contours of the annulus is obtained at the level of the annulus (**c**). *AoR* aortic root, *LA* left atrium, *LVOT* left ventricular outlet tract, *RA* right atrium

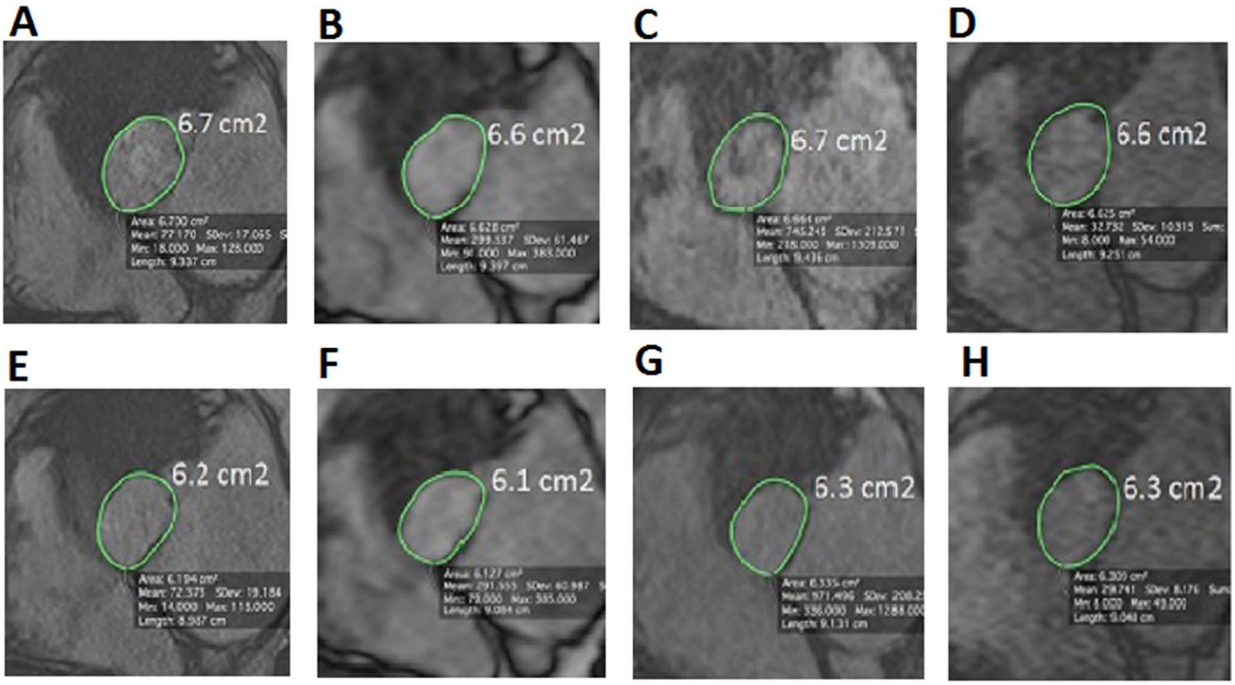

Fig. 4.

Comparison of aortic annulus area between the different MR sequences. Aortic annulus area measured with the different MR sequences in an 80 year old TAVR candidate subject during systole (top images) and diastole (bottom images) using 2D cine b-SSFP (**a**, **b**), 3D cine b-SSFP (**b**, **f**), navigator triggered 3D b-SSFP MRA (**c**, **g**) and k–t accelerated 3D cine b-SSFP (**d** and **h**). We can appreciate in this figure the similarity in the aortic annular area value between the k-t accelerated 3D cine b-SSFP and the other conventional MR techniques during both systolic and diastolic phases

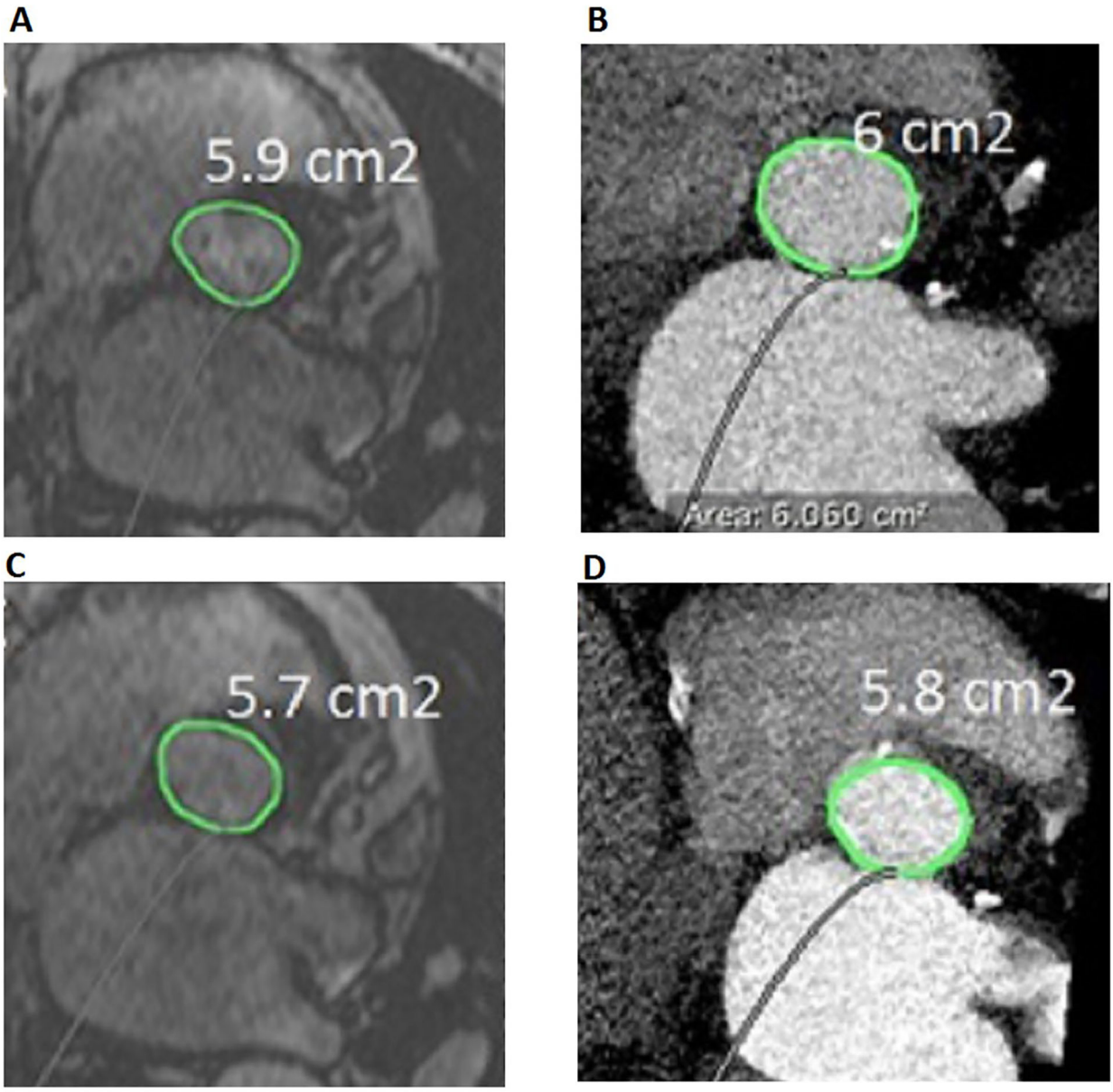

Fig. 5.

Comparison of aortic annulus area between k–t accelerated 3D cine b-SSFP and CTA. Aortic annulus area measured from k–t accelerated 3D cine b-SSFP (**a** during systole and **c** during diastole) and CTA (**b** during systole and **d** during diastole) in a 65 year old TAVR candidate subject

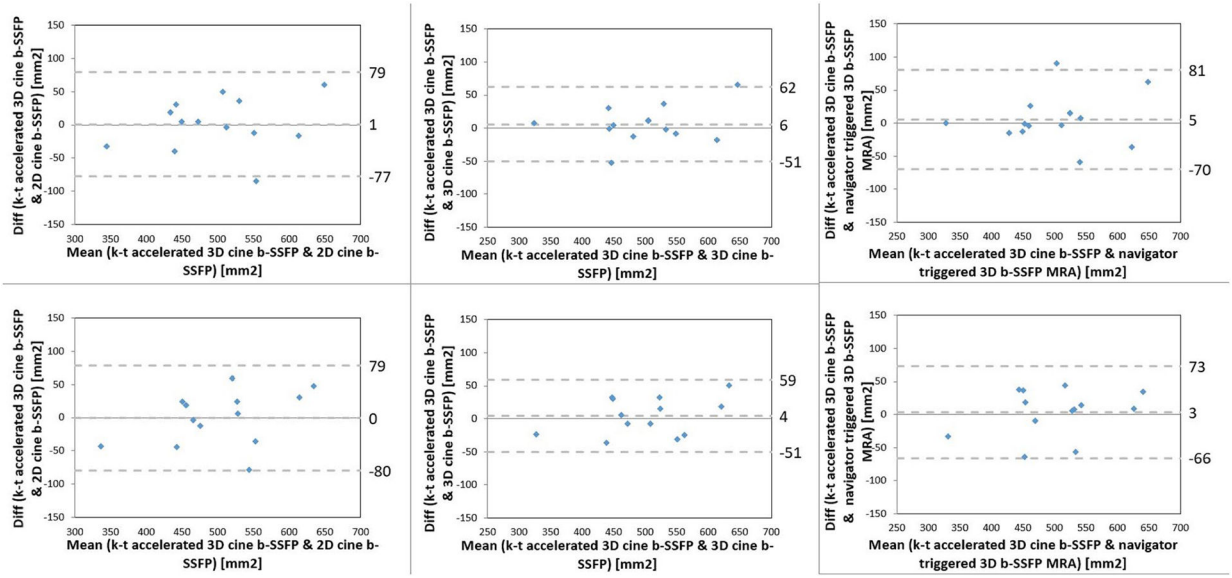

Fig. 6.

Bland-Altman analysis comparing systolic aortic annular area by k–t accelerated 3D cine b-SSFP to each of the conventional non-contrast MRI techniques (2D cine b-SSFP, 3D cine b-SSFP, navigator-triggered 3D b-SSFP MRA) by both raters (rater 1 top row, rater 2 bottom row)

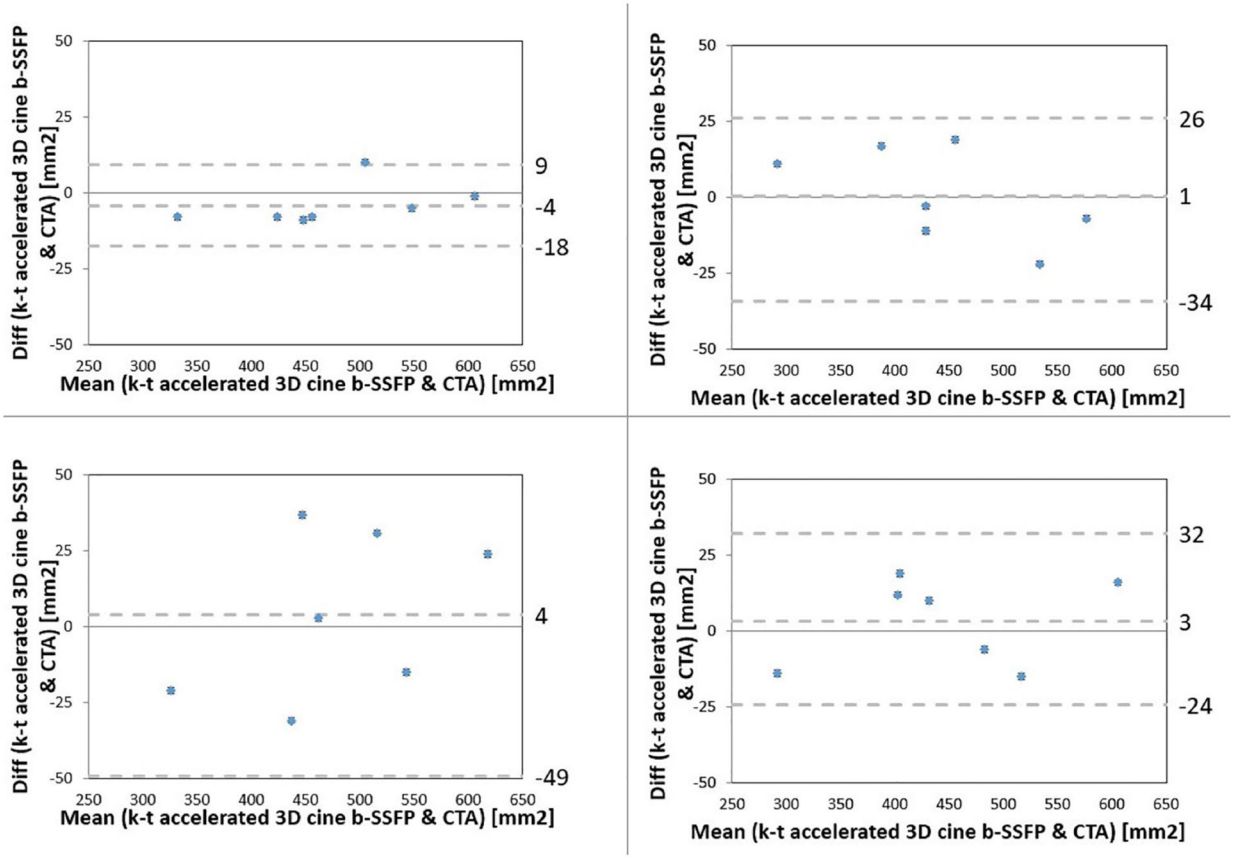

Fig. 7.

Bland–Altman analysis comparing systolic (left column) and diastolic (right column) aortic annular area by k–t accelerated 3D cine b-SSFP to CTA by both raters (rater 1 top row, rater 2 bottom row)

Table 1

Typical parameters for each of the MRI sequences

	2D cine b-SSFP	3D cine b-SSFP	Navigator triggered 3D b-SSFP MRA	k–t accelerated 3D cine b-SSFP
Field of view (mm^2)	360×302	340×273	440×303	340×298
Acquired spatial resolution (mm^3)	0.9×1.1×5	1.8×2.4×6.7	1.4×1.5×2	1.5×2.7×1.5
Interpolated spatial resolution (mm^3)	0.9×0.9×5	0.9×0.9×5	1.4×1.4×1.4	1.5×1.5×1.5
Length of coverage (mm)	15 (5 mm slice thickness × 3 slices)	29	38.6	24
Temporal resolution (ms)	62.8	54.3	287.9	91
Cardiac phases	25 (calculated phases)	11	1	8
Averages	2	1	1	1
TR/TE	3.5/1.44	2.9/1.22	3.5/1.46	3.5/1.7
Flip angle	74	60	90	90
Bandwidth (Hz/Px)	893	898	601	1170
Acceleration factor	2	2	2	5
Time of acquisition (s)	51 (17 sec per slice × 3 slices)	20	122	18
Breath-held/ free breathing	Breath-held	Breath-held	Free-breathing	Breath-held

Table 2

Comparison of the conspicuity of aortic annulus and subjective signal to noise ratio

	Rater	Mean values				Friedman test *P* value	Wilcoxon signed ranks test *P* value		
		K–t accelerated 3D cine b-SSFP	2D cine	3D cine	Navigator-triggered 3D b-SSFP MRA		K–t accelerated 3D cine b-SSFP vs 2D cine	K–t accelerated 3D cine b-SSFP vs 3D cine	K–t accelerated 3D cine b-SSFP vs navigator-triggered 3D b-SSFP MRA
Conspicuity	Rater 1	3.3 ± 1.1	4.3 ± 0.6	3.8 ± 0.7	3.3 ± 1.2	0.009	0.011	0.083	0.438
	Rater 2	3.4 ± 0.9	4.2 ± 0.6	3.8 ± 0.7	3.5 ± 1.1	0.017	0.015	0.160	0.666
Image quality	Rater 1	3.1 ± 0.8	4.4 ± 0.7	3.9 ± 1	3.6 ± 1.2	0.001	0.004	0.016	0.144
	Rater 2	3.2 ± 0.8	4.2 ± 0.6	3.9 ± 0.8	3.6 ± 1.2	0.005	0.006	0.026	0.196

Aortic annulus conspicuity and subjective signal to noise ratio were rated as: 1: non diagnostic; 2: marginal; 3: fair; 4: good; 5: excellent. Data is presented as mean ± standard deviation

Table 3

Comparison of annular area (mm^2) measurements in all the subjects

Cardiac phase	k–t accelerated 3D cine b-SSFP	2D cine b-SSFP	*P*	3D cine b-SSFP	*P*	Navigator triggered 3D b-SSFP MRA	*P*
Systole (mean ± SD)	500 ± 88	499 ± 81	0.92	495 ± 76	0.49	495 ± 84	0.62
	503 ± 88	504 ± 73	0.97	499 ± 78	0.60	500 ± 78	0.73
Diastole (mean ± SD)	453.5 ± 77	464.5 ± 92	0.17	453 ± 76	0.89	462 ± 83	0.26
	460 ± 82	457 ± 83	0.58	466 ± 77	0.48	469 ± 78	0.28

Values of annular area measurements are reported as means ± standard deviation in mm^2 (rater 1 top row, rater 2 bottom row) during systolic and diastolic phases for each of the MRI sequences on all the studied subjects (healthy volunteers and TAVR candidates)

Table 4

Comparison of annular area measurements (mm^2) in TAVR candidates

Cardiac phase	k–t accelerated 3D cine b-SSFP	CTA	*P*
Systole (mean ± SD)	472 ± 91	476 ± 87	0.16
	480 ± 99	482 ± 91	0.80
Diastole (mean ± SD)	443 ± 89	443 ± 98	0.93
	449 ± 101	446 ± 98	0.59

Values of annular area measurements are reported as means ± standard deviation in mm^2 (rater 1 top row, rater 2 bottom row) during systolic and diastolic phases for k–t accelerated 3D cine b-SSFP and for CTA in TAVR candidates

Table 5

Inter-rater agreement on qualitative analysis

	Conspicuity		Image quality	
	Kappa	**95% confidence interval**	**Kappa**	**95% confidence interval**
K-t accelerated 3D cine b-SSFP	0.685	0.391–0.979	0.882	0.659–1.000
2D cine	0.711	0.348–1.000	0.594	0.210–0.978
3D cine	0.717	0.368–1.000	0.774	0.502–1.000
Navigator-triggered 3D b-SSFP MRA	0.896	0.700–1.000	1.000	1.000–1.000